Eur. Phys. J. B **3**, 203–209 (1998)

**THE EUROPEAN PHYSICAL JOURNAL B**



# Undulation instability in two-dimensional foams of magnetic fluid

F. Elias[1,a], I. Drikis[1,2], A. Cebers[2], C. Flament[1], and J.-C. Bacri[1]

[1] Université Paris 7, Denis Diderot, Unité de Formation et de Recherche de Physique (case 70.08), 2 place Jussieu, 75251 Paris Cedex 05, France
and
Laboratoire des Milieux Désordonnés et Hétérogènes (case 78), Université Paris 6[b], 4 place Jussieu, 75252 Paris Cedex 05, France

[2] Institute of Physics, Latvian Academy of Sciences Salaspils 1, 2169 Riga, Latvia

Received: 13 October 1997 / Received in final form: 28 January 1998 / Accepted: 9 March 1998

**Abstract.** Two-dimensional magnetic fluid foams are cellular structures whose framework is made of magnetic fluid. The features of these equilibrated patterns are driven by a control parameter: the amplitude of the applied magnetic field. When the latter is rapidly increased, an instability occurs: the walls between cells undulate. Such an instability has also been observed in other 2D cellular structures, which exist for instance in Langmuir monolayers or in magnetic garnets thin films. In this paper we give a theoretical analysis of this instability, the issues of which are shown to be well confirmed by experiments and numerical simulations.

**PACS.** 75.50.Mm Magnetic liquids – 46.30.Lx Static buckling and instability

## 1 Introduction

Bubble, foam and stripe patterns are present in a wide variety of dipolar systems, like ferromagnetic films, amphiphile monolayers, plane layers of magnetic fluid [1]. These equilibrium structures are due to the balance between attractive interactions and repulsive dipolar interactions. In a plane layer of magnetic fluid (MF) submitted to a perpendicular homogeneous magnetic field, the competition between the surface energy and the long-range magnetic dipole-dipole interaction leads to the formation of such patterns at the millimetric scale. A complete review of these two-dimensional (2D) patterns is given elsewhere [2].

In [3,4] the author has established the smectic-like behaviour of the 2D MF stripe system. The elastic constants of this macroscopic 2D smectic have been measured and calculated [5]. A quasi-static increasing of the applied magnetic field leads to an undulation of the stripes, and to the formation of a chevron pattern for high values of the magnetic field [5]. In reference [6] the dynamics and the instabilities of an isolated stripe have been studied. For a given value of the ramp rate of the magnetic field a fingering phenomena occurs for a thick stripe, while a bending phenomena occurs for a thin stripe. Finally the stripe relaxes in order to reach its equilibrium state.

A similar behaviour, as it will be illustrated below, can also be expected in 2D foams of MF [7], with cell boundaries made of MF stripes which join at vertices. Indeed the width of these boundaries is fixed by the control parameters, which are, $H_0$, the amplitude of the external field, $h$, the thickness of the layer, and $\Phi$, the volume fraction of MF. As in the case of the MF stripes, the thickness decreases if the strength of the applied magnetic field is increased, then the total length of the MF boundaries must be increased. Therefore, if the magnetic field is rapidly increased, the global rearrangements of the stripe network in the foam have no time to occur, and the MF stripes undulate. This phenomenon is experimentally and numerically illustrated below. Such an instability has also been observed in other 2D cellular structures. In magnetic garnet thin films, a froth is obtained if a perpendicular magnetic field is applied. The pattern consists in bubbles which are domains of magnetization parallel to the applied field, surrounded by a domain the magnetization of which is antiparallel to the field [8,9]. A buckling of the cell edges occurs on decreasing the amplitude of the magnetic field: the size of the global framework is then increased for the system to decrease its total magnetization. A 2D foam pattern can also be formed in amphiphile monolayers at the air-water interface [10]. In the coexistence region of the phase diagram between a 2D liquid phase and a 2D gaseous phase, cells made of the gaseous phase surrounded by the liquid phase are observed. The network undulates if the temperature is rapidly increased near the critical point. It is reasonable to assume that this phenomenon is caused by the same reasons which account for the undulation instability in the 2D MF foams. Let us also remark

[a] e-mail: elias@aomc.jussieu.fr

[b] URA 800 du CNRS

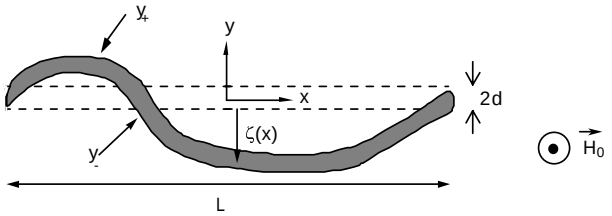


**Fig. 1.** Sketch representing a top view of a stripe with the notations used for the calculation of the energy of an isolated long stripe.

that a similar analysis can also explain the quite complicated dynamics of the networks observed in a recent numerical simulation for the labyrinthine instabilities of a MF droplet [11].

## 2 Theoretical analysis

In this calculation we consider the foam as an assembly of isolated stripes, which are linked one to each others by vertices (the coordination number is always equal to three). The vertices are fixed because the time of variation of the external magnetic field is smaller than the time of vertices displacements. Let us then consider one MF stripe of length, $L$, with a fixed volume, confined between two plates separated by a distance $h$. The notations used in this calculation are shown in Figure 1. The energy of the stripe includes an interfacial energy and a magnetic energy. The demagnetizing field energy of the stripe can be expressed as follows [12]:

$$E_{dm} = -\frac{\mu_0}{2}\int_{V_{MF}} dV\,\mathbf{M}\cdot\mathbf{H}_d = \frac{\mu_0}{4\pi}\mathbf{M}^2\int_{S_{MF}} d^2\rho\int_{S_{MF}} d^2\rho'\left[\frac{1}{|\rho-\rho'|}-\frac{1}{\sqrt{(\rho-\rho')^2+h^2}}\right] \tag{1}$$

where the MF magnetization $\mathbf{M}$ is supposed to be constant within the stripe and parallel to the external magnetic field and $\mathbf{H}_d$ is the demagnetizing field. The integration in (1) is carried out along the MF-oil interface in the $(x, y)$ plane (see Fig. 1). equation (1) can be obtained by the surface charge analogy [4], which transforms the dipolar-dipolar potential into a Coulombic potential between magnetic charges on the upper and lower boundaries of the MF layer. The surface tension forces of the MF-oil interfaces must be accounted for. The equations of the stripes boundaries $y_+$ and $y_-$ are: $y_+ = d + \zeta(x)$ and $y_- = -d + \zeta(x)$ (Fig. 1). The interfacial energy of a slightly deformed stripe can thus be expressed as follows:

$$E_s = 2\sigma h\int_{-\frac{L}{2}}^{\frac{L}{2}} dx\sqrt{1+\zeta'^2(x)}, \tag{2}$$

where $\sigma$ is the MF-oil surface tension. We use here the usual and reasonable assumptions [12–14], that the MF-oil interfaces are normal to the plane of the layer. The total energy of the stripe is then calculated up to the second order term in the undulation amplitude, $\zeta(x)$, neglecting the end effects. It is expressed as follows:

$$E = 2\sigma hL + \sigma h\int \zeta'^2(x)dx + \frac{\mu_0}{4\pi}LM^2h^2D\left(\frac{2d}{h}\right) - \frac{\mu_0}{4\pi}M^2\int dx\int dx'\,[\zeta(x')-\zeta(x)]^2 \times\left[\frac{1}{\sqrt{(x-x')^2}}-\frac{1}{\sqrt{(x-x')^2+h^2}} -\frac{1}{\sqrt{(x-x')^2+(2d)^2}} +\frac{1}{\sqrt{(x-x')^2+(2d)^2+h^2}}\right], \tag{3}$$

where

$$D\left(\frac{2d}{h}\right) = \left(\frac{2d}{h}\right)^2\ln\left[1+\left(\frac{h}{2d}\right)^2\right] - \ln\left[1+\left(\frac{2d}{h}\right)^2\right] + 4\frac{2d}{h}\arctan\left(\frac{2d}{h}\right). \tag{4}$$

For a straight stripe, $N = 2(h/2d)D(2d/h)$ is the demagnetizing factor.

Representing the bending deformation by a Fourier integral $\zeta(x) = \frac{1}{2\pi}\int\zeta(k)e^{ikx}dk$, equation (3) in the limit $L\to\infty$ gives:

$$E = 2\sigma hL + \frac{\mu_0}{4\pi}LM^2h^2D\left(\frac{2d}{h}\right) + \frac{\sigma}{2\pi h}\int|\zeta(k)|^2 f_e(k)dk \tag{5}$$

where:

$$f_e(k) = (kh)^2 - 4B_m\left[\ln\left(\frac{kh}{2}\right) - \frac{1}{2}\ln\left(1+\left(\frac{h}{2d}\right)^2\right) + \gamma + K_0(kh) + K_0(2kd) - K_0\left(k\sqrt{(2d)^2+h^2}\right)\right]. \tag{6}$$

$K_0$ is the Mc Donald function, $\gamma$ the Euler constant and $B_m = \frac{\mu_0}{4\pi}\frac{M^2h}{\sigma}$, the magnetic Bond number.

The two first terms in equation (5) represent the energy of a straight stripe. The third term is the deformation energy of the stripe: the deformation occurs if this term is negative, whereas the stripe remains straight if it is positive or zero. Hence according to equation (5), the undulation of the stripe is energetically allowed if the spectral density of the undulation energy, $f_e(k)$, given by equation (6), is negative. The stripe shape is then the result of the superimposition of all the wavelengths $\lambda = 2\pi/k$ for which

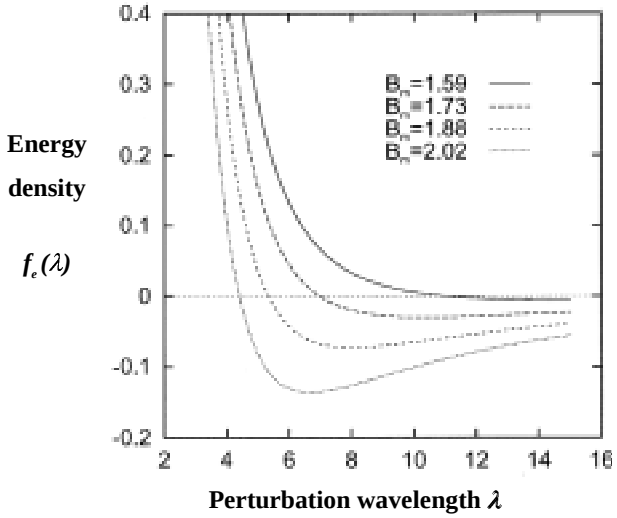


**Fig. 2.** Spectral density of the undulation energy, $f_e(\lambda)$, for magnetic Bond numbers $B_m = \frac{\mu_0}{4\pi}\frac{M^2 h}{\sigma} = 1.59$, 1.73, 1.88 and 2.02. These values correspond, according to equation (10), to an effective surface tension $\sigma_e/\sigma = -0.1$, $-0.2$, $-0.3$ and $-0.4$. The undulation is allowed when the deformation energy of the stripe is negative, *i.e.*, according to equation (5), when the function $f_e(\lambda)$, given by equation (6), becomes negative. This occurs for the large wavelength modes. The minimal allowed undulation wavelength, $\lambda_{min}$, diminishes when $B_m$ is increased. In a foam, where an undulation occurs if the MF walls length is at least equal to one allowed wavelength, it means that there exists a critical value of $B_m$ for the stripes undulation: the shorter the stripe, the higher $B_{m_c}$. The minimum of $f_e(\lambda)$ determines the energetically most favorable bending mode. The wavelength are given in units of the experimental cell thickness $h$ ($h = 1$ mm in the experiments).

$f_e(k) < 0$. This is the crucial point for the understanding of the present analysis. Moreover, the minimum of $f_e(k)$ determines the most energetically dangerous bending deformation mode, for a given value of the magnetic Bond number. The function $f_e(k)$ is plotted in Figure 2 *versus* the undulation wavelength $\lambda = 2\pi/k$ for $B_m = 1.59$, 1.73, 1.88, 2.02 and $2d/h = 1.0$. These curves show that the allowed wavelength bending deformation modes are the longest ones for the lowest values of $B_m$. When $B_m$ is increased, the minimal value of $\lambda$ (which is the root of $f_e(\lambda) = 0$ given by Eq. (6)), $\lambda_{min}$, diminishes. In a foam, the length of a stripe is limited by two vertices. The undulation deformation will thus develop if the length of the stripe, $L$, is at least greater than one allowed wavelength. For a given magnetic Bond number, the stripes for which $L > \lambda_{min}$ undulate, and those for which $L < \lambda_{min}$ remain straight. As a result of this theoretical analysis, the magnetic Bond number must be greater than some critical value for the MF boundaries to undulate in a foam. This critical value of $B_m$ is different for each MF wall, and depends on the length of the stripe. This result is experimentally and numerically confirmed below. The growth increments for a viscous magnetic fluid stripe deformation in dependence on the wave number of the undulation are calculated in reference [15].

The phenomenon of bending instability of a MF stripe can also be understood in the following qualitative way, using the argument of negative effective surface tension. The equilibrium width of the long straight stripe is found minimizing the two first terms of the right side of equation (5) with respect to $2d/h$, for a fixed stripe area $S = 2dL$. Using equation (4), it gives the following equation:

$$B_m \left[ \left(\frac{2d}{h}\right)^2 \ln\left(1 + \left(\frac{h}{2d}\right)^2\right) + \ln\left(1 + \left(\frac{2d}{h}\right)^2\right)\right] = 2. \tag{7}$$

Expanding $f_e(k)$ up to the second order terms in the wave number $k$ using equation (6), the expression (5) in the limit of the long wavelength deformations can be written as follows:

$$E = 2\sigma h L + \frac{\mu_0}{4\pi} L M^2 h^2 D\left(\frac{2d}{h}\right) + \sigma_e \frac{h}{2\pi}\int |\zeta(k)|^2 k^2 dk, \tag{8}$$

where

$$\sigma_e = \sigma\left(1 - \frac{1}{2}B_m\left[\left(\frac{2d}{h}\right)^2 \ln\left(1 + \left(\frac{h}{2d}\right)^2\right) + \ln\left(1 + \left(\frac{2d}{h}\right)^2\right)\right]\right). \tag{9}$$

Therefore $\sigma_e = \sigma f_e(k)/(hk)^2$ acts as an effective surface tension, which does not depend on $hk$ in the limit $hk \to 0$. From equation (7), one can see that $\sigma_e$ is exactly equal to zero if the stripe width reaches its equilibrium value. Moreover, the equilibrium width, $2d$, of a long straight stripe is a decreasing function of the magnetic Bond number. Thus because the total area of the stripe is fixed, the equilibrium length of the stripe increases with an increasing $B_m$. If $B_m$ is rapidly increased, the stripe has no time to reach its equilibrium length. Therefore its width becomes bigger than its equilibrium value; according to equation (9) the effective surface tension $\sigma_e$ becomes negative and the stripe must undulate.

Stripe undulation is also observed in 2D foams of ethyl heptadecanoate monolayers [10] or porphyrin monolayers [16], in the coexistence region of the phase diagram between a 2D gaseous phase and a 2D liquid phase. It occurs if the temperature is fast enough risen at the right side of the critical point [10]. This instability can also be explained rather well by the action of dipolar forces (with a fast temperature increasing), using equation (6). Since for foams of amphiphile monolayers the distance $h$ between opposite charges is quite small in comparison with the width of the stripes, the parameter $2d/h$ is large. In this case, the Bond number is defined as $\mu^2/\gamma$ [17], where $\mu$ is the electric dipole moment surface density, and $\gamma$ is the line tension between the two phases. According to equation (7), the critical Bond number for the undulation deformation is

$$B_{m_c} \approx \frac{1}{\ln(2d/h)}\,. \tag{10}$$

According to the relation (6), the wave number $k_0$ of the energetically most favorable undulation deformation can be expressed for the asymptotic relation valid at $B_m \to 0$ and $kh \to 0$:

$$hk_0 = 2\exp(-1/B_m). \tag{11}$$

From relations (10, 11) it follows a simple estimation for the wavelength of the energetically most favorable undulation deformation mode ($B_m > B_{m_c}$): $\lambda \geq \lambda_m = \pi d$. The last estimation for the wavelength of the undulation deformations at $2d = 3$ $\mu$m [10] gives $\lambda \geq 10$ $\mu$m, what is fairly in good accordance with the wavelength of the undulation deformations observed in experiments. The values of the critical Bond number obtained from equation (11) for $2d = 3$ $\mu$m and $h = 3$ Å, $B_{m_c} \approx 0.11$, looks also quite reasonable in comparison with other amphiphile systems referenced in [18] ($B_{m_c} \approx 0.03$) and in [19] ($B_{m_c} \approx 0.08$), as obtained from the shape thermal fluctuation studies of 2D droplets in amphiphile monolayers [20].

## 3 Experimental results

A MF, also called ferrofluid, is a colloidal suspension of nanoscopic ferromagnetic particles. Here we use an ionic MF (water based) with cobalt ferrite particles [21].

Our system consists in a mixture of a MF and an immiscible oil of lower density. This mixture is placed in a cell made of Altuglass©, the thickness is very small ($h = 1$ mm) in comparison with the other dimensions (*ca.* 10 cm). The presence of the oil avoids wetting phenomena of the MF, because a thin film of oil always lies between the MF and the walls. The cell is placed in the horizontal position and located between two coils in the Helmholtz configuration, in order to get a vertical spatially homogeneous magnetic field. An alternating magnetic field $H(t) = H_0\cos(2\pi\nu t)$ (frequency $\nu = 50$ Hz) is required to create a MF foam pattern, which consists of cells of oil separated by MF boundaries, as it is extensively described in [7]. The images are recorded by a video camera and digitized in a computer. An increase in $H_0$ involves an increase in the MF magnetization, and thus an increase in the magnetic Bond number. The MF volume fraction $\Phi$ fixes the mean length of the MF stripes in the foam: $\langle L\rangle \approx 3(1/\Phi - 1)2d$. Since the dispersion of the MF stripe length around $\langle L\rangle$ is small, the experiments have been performed for two different values of $\Phi$. $\Phi = 0.04$ ($\langle L\rangle = 22.5$ mm) and $\Phi = 0.20$ ($\langle L\rangle = 6.4$ mm). Figure 3 shows the undulation instability for $\Phi = 0.20$. The experiment has been done rapidly (the ramp rate of the magnetic field is $dH/dt = 0.22$ $\mathrm{Am^{-1}s^{-1}}$), so the vertices have no time to move, and the assumption of fixed vertices is quite reasonable. One can also see in Figure 3 that the longest MF walls undulate first on increasing $B_m$, and the shortest stripes do not undulate. Let us notice that a characteristic distance between stripes appears in Figure 3c, suggesting that the interactions between stripes are important for high values of the magnetic Bond number. Nevertheless for this value of $B_m$, only the shortest stripes remain straight.

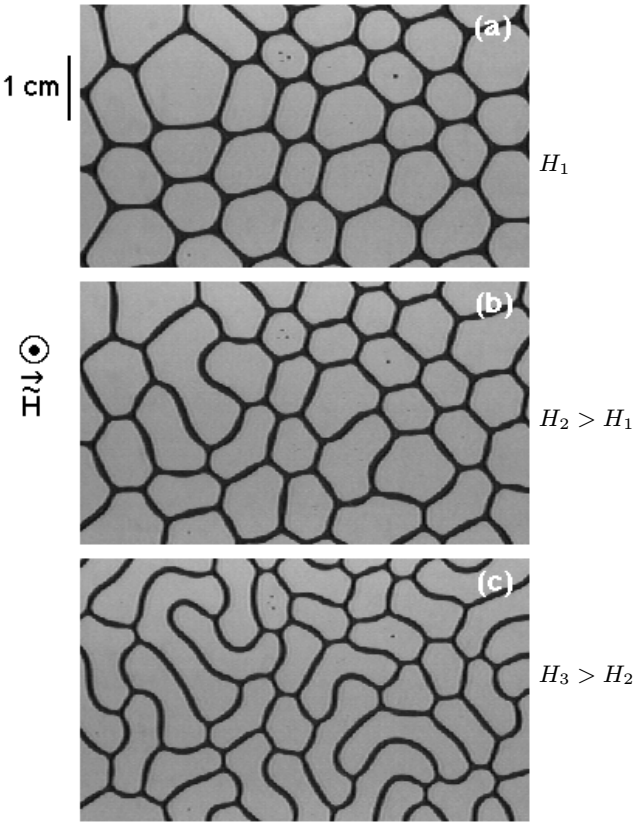


**Fig. 3.** Photographs of the undulation instability. The MF appears black. The MF volume fraction is $\Phi = 0.20$. The initial magnetic Bond number at $t = 0$ is equal to 1.2, then it is increased with a growth rate of $4 \times 10^{-3}$ $\mathrm{s^{-1}}$ (corresponding to $dH/dt = 0.22$ $\mathrm{Am^{-1}s^{-1}}$). (a) $t = 115$ s and $B_m = 1.9$; the magnetic Bond number is just below its critical value for the MF stripes to undulate in such a foam, and no stripe is bent. (b) $t = 125$ s and $B_m = 2.0$; the longest walls begin to undulate. (c) $t = 190$ s and $B_m = 2.2$; the bending instability is well developed for the most of the stripes, but the shortest ones remain straight.

Most of the stripes in the foam begin undulating for lower values of $B_m$; in this case the aspect of the foam is like in Figure 3b: no characteristic length scale appears so clearly as in Figure 3c, suggesting that the stripe-stripe interactions are weak. The model is thus expected to be valid only for the low values of $B_m$. Figure 4 shows the experimental data corresponding to the wavelength of the MF walls at the threshold of their undulation *versus* $B_{m_c}$. These data are fitted with the theoretical curve obtained from equation (6): $f_e(k = 2\pi/\lambda, B_{m_c}) = 0$, with a fixed value of the stripes width: $2d = 0.83$ mm, which corresponds to the measured one. The MF/oil surface tension has been taken as a fitting parameter. One obtain $\sigma = (22 \pm 2)$ $\mathrm{mNm^{-1}}$; comparable values have been already measured in previous works [5,7]. The accordance between the experimental data and the theoretical predictions validates the model of the bending instability presented here, in spite of the strong assumptions. That conclusion is further supported

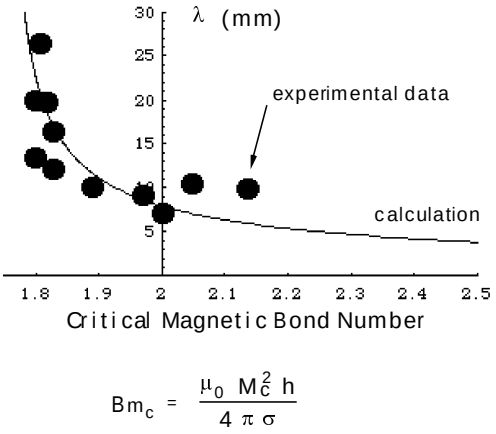


**Fig. 4.** Comparison between the theory and the experiments. The wavelength of the MF walls undulation at the threshold of the instability have been plotted *versus* the corresponding critical magnetic Bond number. A fit of these data is obtained from equation (6), with $f_e(k = 2\pi/\lambda,\, B_m = B_{m_c}) = 0$ at the threshold of the instability, for $2d = 0.83$ corresponding to the measured width of the MF stripes.

by the results of the numerical simulations described in the next section.

Let us notice that, contrary to the bending stripe instability in the 2D MF smectic system [3–5], the wall undulation in a MF foam is a dynamical effect. Indeed, after some long time the bending disappears, because of the foam rearrangements which consist in two facts: on one side the MF flow through the vertices is responsible of the vertex motion; on another side the cells of the foam can grow or shrink by oil flow between the MF and the plates of the Hele-Shaw cell. The time scales are the following: the response time of the undulating MF walls is of the order of 1 s and the response time of the vertices is about several min. The growth rate of the cell area is of the order of $10^{-2}$ mm$^2$s$^{-1}$. Since an experiment lasts for about 5 min, the vertex motions and the variation of the cell area can be neglected. Nevertheless they are responsible for the long time relaxation of the pattern. Furthermore for high values of the magnetic Bond number the foam is destroyed: the MF boundaries come off the vertices; the final pattern is one long MF stripe, meaning that this pattern is more stable than the network structure (*i.e.* the foam is a metastable pattern in comparison with the stripe pattern).

## 4 Numerical simulations

The numerical method is based on a boundary integral equation formulation for the Hele-Shaw flow of the MF, described by the modified Darcy equation due to the action of the MF selfmagnetic forces [15,22]:

$$-\alpha v - \nabla p + \frac{2M}{h}\nabla\varphi = 0;\ \text{div}\ v = 0, \qquad (12)$$

where $v$ is the local velocity of the MF, $p$ is the pressure, and $\alpha$ is a constant which depends on the MF viscosity and on the cell thickness $h$. The magnetostatic potential for the particular configuration of the MF, $\varphi(\rho)$, is expressed as follows under the assumption of uniform magnetization:

$$\varphi(\rho) = -M \int d^2\rho \left[\frac{1}{|\rho - \rho'|} - \frac{1}{\sqrt{(\rho - \rho')^2 + h^2}}\right]. \qquad (13)$$

The pressure at the interface is determined according to the Laplace law:

$$(P)_{L_i} = \sigma\kappa_i, \qquad (14)$$

where $\kappa_i$ is the radius of curvature of the interface and $L_i$, $i = 1, ..., N_c$, are the foam interfaces. For the boundary integral equation formulation of the problem (12, 14), the stream function of the potential 2D flow $\left(v_x = \frac{\partial\Psi}{d_y};\ v_y = -\frac{\partial\Psi}{\partial_x}\right)$ satisfying Laplace equation is expressed as a simple layer potential:

$$\Psi = \frac{1}{2\pi}\sum_{i=1}^{N_c} \int dl' f_i(l') \ln(|\rho - \rho'|). \qquad (15)$$

According to the relations (12, 14), the tangential component of the velocity of the fluid on the interfaces is known and is expressed as follows: $v_t = -\frac{1}{\alpha}\left[\frac{d}{dl}\left(\sigma\kappa - \frac{2M}{h}\varphi\right)\right]$. The normal derivative of the stream function on the boundary is: $\frac{\partial\Psi}{\partial n} = -v_t$. Then taking into account the theorem for normal derivative of the simple layer potential, the following set of equations for the functions $\{f_i\}$ is obtained:

$$-2\left[\frac{d}{dl}\left(\kappa - \frac{2B_m}{h^2}\varphi(l)\right)\right]_{L_i} = f_i(l) - \sum_{j=1}^{N_c}\frac{A_j}{\pi} P\oint_{L_j} f_j(l')\frac{y_l(x - x') - x_l(y - y')}{(x - x')^2 + (y - y')^2}dl' \qquad (16)$$

where $A_i = -1$ for all the interfaces of the foam except the external boundaries ($i = 1$), for which $A_i = 1$. $x(l)$ and $y(l)$ are parametric representations of the foam interfaces, $x_l$ and $y_l$ are derivatives of the parametric representations, and $P$ denotes the Cauchy principal value. For the simplicity of the numerical calculations, the expression of the magnetostatic potential (13) is transformed into a contour integral [14,22]:

$$[\varphi(l)]_{L_i} = -A_i\sum_{j=1}^{N_c} A_j \oint_{L_j}\left(\frac{x_l'(y - y') - y_l'(x - x')}{\sqrt{(x - x')^2 + (y - y')^2}} - x_l \ln\left(y - y' + \sqrt{(x - x')^2 + (y - y')^2 + h^2}\right)\right)dl'. \qquad (17)$$

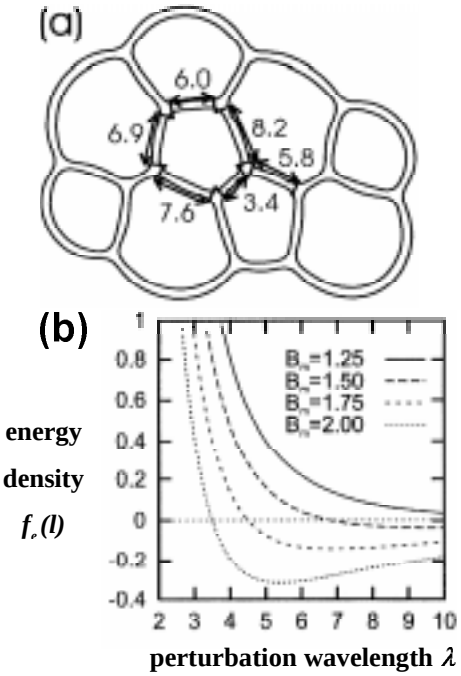


**Fig. 5.** (a) MF foam which has been used as the initial configuration of the numerical simulations. The indicated lengths of the walls are given in units of the experimental cell thickness $h$. (b) Energy density $f_e(k = 2\pi/\lambda)$ *versus* the perturbation wavelength (in units of $h$) at different magnetic Bond numbers $B_m$. For this foam, $\langle 2d \rangle = 1.2h$.

The Cartesian components of the velocity $a$ the interfaces, $[(v_{x'}\ v_y)]_{L_i}$, are then calculated:

$$[(v_x,\ v_y)(l)]_{L_i} = \frac{f_i(l)(x_l, y_l)}{2(x_l^2 + y_l^2)} + \frac{1}{2\pi}\sum_{j=1}^{N_c} P \oint_{L_j} f_j(l') \frac{(y - y',\ -x + x')}{(x - x')^2 + (y - y')^2} dl'. \quad (18)$$

The numerical methods based on an energetic approach [23] are not useful in this case, because the undulation is a dynamical effect out of equilibrium. The numerical method presented here takes account of the magnetic interactions in a more realistic way, *i.e.* we account for the dipole-dipole interactions exactly by solving (in approximation of constant magnetization) the Maxwell equations. The cell size is conserved in the present boundary integral equation formulation, because the bubble growth can be neglected in one experiment (see the experimental time scales given in Part 3).

The numerical simulations have been performed for the given configuration of the MF foam shown in Figure 5a. The average MF walls thickness is $\langle 2d \rangle = 1.2h$. This value is estimated from the relation $\langle 2d \rangle = 2S/\mathcal{L}$, where $S$ is the total area of MF domain, and $\mathcal{L}$ is the total length of all the interfaces. $S$ and $\mathcal{L}$ can be easily determined from the numerical data. The values of some wall lengths (in units of cell thickness), $L/h$, are also indicated in Figure 5a. They must be at least greater than one wavelength for the development of the undulation deformations. The equilibrium for this given foam according to equation (7) corresponds to $B_m = 1.2$. The spectral density of the undulation energy *versus* the perturbation wavelength, $f_e(\lambda)$, is plotted in Figure 5b, for some values of $B_m$. According to the relation (5), only the modes with $f_e(\lambda) < 0$ are growing. To satisfy this condition, stripes with enough large length for given $B_m$ must be present in the foam. We can see that for $B_m = 1.25$, all stripes in the foam should be stable. For $B_m = 1.5$, only the longest walls ($L/h = 7.6$ and $L/h = 8.2$) can undulate, but for $B_m = 1.75$ most of the stripes should be undulated. The results of the numerical calculations presented in Figure 6 correspond to the expectations reasonably well. That means that the model of the infinite stripe works quite well for the foam with enough large ratio $L/d$ (Fig. 5a).

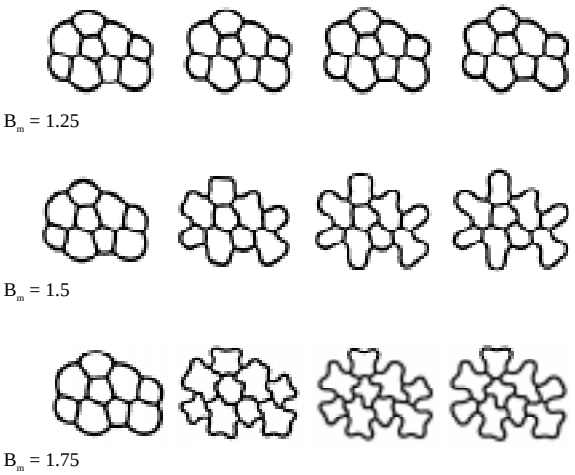


**Fig. 6.** Results of the numerical simulations. MF foam structure when increasing the time (from left to right), for magnetic Bond number $B_m = 1.25$ (upper row), $B_m = 1.5$ (middle row) and $B_m = 1.75$ (lower row).

## 5 Conclusions

In this paper, we give a theoretical analysis of the undulation instability, which occurs in a two-dimensional magnetic fluid foam if the strength of the applied magnetic field is increased fast enough. It is a dynamical (out of equilibrium) effect. The calculation is performed for an isolated stripe; we consider the whole foam as an assembly of isolated magnetic fluid stripes, linked one to each other by fixed vertices. We show that a critical value of the magnetic Bond number exists, above which a magnetic fluid stripe undulates in the foam. This critical value depends on the stripe length; the shorter the stripe, the higher the critical value of $B_m$. These theoretical predictions are well confirmed by experiments and by numerical simulations.

Such a calculation can be extended to account for undulation instability in other 2D cellular structures which are driven by the competition between surface energy and dipolar repulsive interactions, for instance 2D foams in amphiphile monolayers.

## References


1. M. Seul, D. Andelman, Science **267,** 476 (1995).
2. F. Elias, C. Flament, J.-C. Bacri, S. Neveu, J. Phys. I France **7,** 711 (1997).
3. A. Cebers, Magnitnaya Gidrodinamica **30,** 179 (1994); Magnetohydrodynamics **30,** 148 (1994).
4. A. Cebers, J. Mag. Mag. Mat. **149,** 93 (1995).
5. C. Flament, J.-C. Bacri, A. Cebers, F. Elias, R. Perzynski, Europhys. Lett. **34,** 225 (1996).
6. J.-C. Bacri, A. Cebers, C. Flament, S. Lacis, R. Melliti, R. Perzynski, Progr. Colloid Polym. Sci. **98,** 30 (1995).
7. F. Elias, C. Flament, J.-C. Bacri, O. Cardoso, F. Graner, Phys. Rev. E **56,** 3310 (1997).
8. K.L. Babcok, R.M. Westervelt, Phys. Rev. A **40,** 2022 (1989).
9. M. Portes de Albuquerque, P. Molho, J. Mag. Mag. Mat. **113,** 132 (1992).
10. K.J. Stine, Ch.M. Knobler, R.C. Desai, Phys. Rev. Lett. **65,** 1004 (1990).
11. A. Cebers, I. Drikis, Magnitnaya Gidrodinamica **32,** 11 (1996); Magnetohydrodynamics **32,** 8 (1996).
12. A. Cebers, M.M. Maiorov, Magnitnaya Gidrodinamica **16,** 27 (1980); Magnetohydrodynamics **16,** 21 (1980).
13. S.A. Langer, R.E. Goldstein, D.P. Jackson, Phys. Rev. A **46,** 4894 (1992).
14. D.P. Jackson, R.E. Goldstein, A. Cebers, Phys. Rev. E **50,** 298 (1994).
15. A. Cebers, Magnitnaya Gidrodinamica **17,** 3 (1981); Magnetohydrodynamics **17,** 113 (1981).
16. M. Yoneyama, A. Fuji, S. Maeda, T. Murayama, J. Phys. Chem. **96,** 8982 (1992).
17. A. Cebers, Magnitnaya Gidrodinamika **25** 13 (1989); Magnetohydrodynamics **25,** 149 (1989).
18. D.J. Benvegnu, H.M. Mc Connell, J. Phys. Chem. **96,** 6820 (1992).
19. E. Goldstein, D.P. Jackson, J. Phys. Chem. **98,** 9626 (1994).
20. M. Seul, Physica A **168,** 198 (1990).
21. S. Neveu-Prin, F.A. Tourinho, J.-C. Bacri, R. Perzynski, Colloid Surf. A **80,** 1 (1993).
22. A. Cebers, Magnitnaya Gidrodinamika **20**, 43 (1984); Magnetohydrodynamics **20,** 140 (1984).
23. D. Weaire, F. Bolton, P. Molho, J.A. Glazier, J. Phys. Condens. Matter **3,** 2101 (1991).